Wind Shear Enhancement of Entrainment and Refractive Index Structure Parameter at the Top of a Turbulent Mixed Layer

C. W. FAIRALL

Department of Meteorology, The Pennsylvania State University, University Park, PA 16802

(Manuscript received 10 May 1984, in final form 16 August 1984)

ABSTRACT

A model for inversion layer turbulence properties of a cloud-free entraining mixed-layer with wind shear at the top is developed. Using the approach of Wyngaard and LeMone (1980), expressions for the average values of ϵ and σ_w^2 in the entrainment region are developed in terms of a mixed layer scaling velocity W_m, the entrainment velocity W_e and several mean profile scaling parameters including the flux Richardson number

$$R_f^{-1} = 7(\Delta S_h)^2 \Gamma T/[6g(\Delta\theta_v)^2],$$

where ΔS_h is the inversion wind shear, Γ the lapse rate of θ_v above the inversion and $\Delta\theta_v$ the buoyancy jump at the inversion. Deardorff's empirical relation for W_e/σ_w is used to close the set of equations and to obtain a parameterization for W_e which applies if R_f is greater than a critical value approximately equal to one-half. The wind shear enhancement of entrainment leads to an increase in the refractive index structure parameter, C_N^2, in the interfacial region. This increase in C_N^2 may be significant under conditions of strong geostrophic forcing combined with a low-level inversion or large baroclinic effects associated with horizontal gradients of mixed-layer temperature or inversion height.

1. Introduction

The mixed layer concept offers a computationally simple (and, therefore, attractive) approach to analyzing and modeling the dynamics of a turbulent boundary layer capped by a temperature inversion. For example, the evolution of the daytime, overland mixed layer (Tennekes, 1973; Stull, 1976) and the stratocumulus topped marine layer (Lilly, 1968; Stage and Businger, 1981; Davidson *et al.*, 1984) have been shown to be reasonably represented by mixed layer models. Such models employ rate equations (Tennekes and Driedonks, 1981) for atmospheric variables including the mixed layer height. The growth of the boundary layer into the nonturbulent, stratified air above is a turbulent process called entrainment. In the classic case of a cloud-free, convectively driven entrainment, the rate of destruction of turbulent kinetic energy at the top of the boundary layer is a fraction (approximately 0.2) of the surface buoyancy flux (Stull, 1976). The additional effects of surface shear production of turbulent kinetic energy can be included with the proper choice of the boundary layer scaling velocity W_m (Tennekes and Driedonks, 1981). For linguistic simplicity this is still referred to as "convectively" driven where both buoyant and forced convection are considered.

This paper is an examination of the effects of moderate wind shear at the inversion (sometimes called the interfacial layer) on the entrainment rate and other turbulence statistics. Inversion wind shear may be important in the cloudfree marine boundary layer where convection is often very weak. A word of caution: this is not considered to be a study of shear *driven* entrainment where the local wind shear dominates the turbulence dynamics, but rather a situation in which shear provides an enhancement of entrainment. The interfacial layer is still controlled by turbulence generated in the boundary layer. Thus, entrainment not only destroys turbulent kinetic energy by pulling down positively buoyant air from above the inversion but also creates kinetic energy by shear production due to the change in mean flow across the inversion. The internal balance of various turbulent kinetic energy production and destruction mechanisms is shifted in a direction favoring a greater entrainment rate. This situation will be explored by considering the budgets of turbulent kinetic energy and vertical velocity variance in the entrainment region.

Turbulent mixed layer concepts have also proven successful in modeling the behavior of the electromagnetic and acoustic refractive index structure parameter C_N^2 (Wyngaard *et al.*, 1971; Wyngaard *et al.*, 1978; Fairall *et al.*, 1982), through its relationship to the fundamental meteorological structure parameters (Gossard, 1960; Friehe *et al.*, 1975; Wesely, 1976)

$$C_N^2 = B(C_T^2 + 2\gamma C_{TQ} + \gamma^2 C_Q^2), \qquad (1)$$

where B and γ are conversion factors that depend on pressure, temperature, wavelength, or type of radiation, C_T^2 is the temperature structure parameter, C_Q^2 the water vapor density structure parameter and C_{TQ} the temperature-humidity structure parameter. Since the entrainment process mixes air parcels of quite different refractive properties, the inversion is a region of importance for wave propagation. Wyngaard and LeMone (1980) have developed a model of inversion layer structure functions for the cloud-free, convective boundary layer. In this paper, Wyngaard and LeMone's model (hereafter referred to as WL) will be extended to the case of an inversion with wind shear.

Several approaches have been taken to obtain entrainment parameterizations in the presence of inversion wind shear. The simplest approach is to ignore the velocity jump at the inversion or to assume that the average effects can be taken into account implicitly in terms of other parameters such as the friction velocity u_* (e.g., Kato and Phillips, 1969). Deardorff and Willis (1982) obtained an empirical relation between the entrainment velocity W_e and the inversion wind shear ΔU from rotating annulus experiments. However, these experiments were done with no convection. Also, the inversion shear was not an explicit independent variable but the result of internal adjustments by the boundary layer and, therefore, highly correlated with u_*. Tennekes and Driedonks (1981) offer a review of the traditional turbulent kinetic energy (TKE) budget approach where the wind shear is explicitly expressed in the shear production terms

$$\overline{uw}\partial U/\partial z = -W_e\Delta U(\Delta U/\Delta h) = -C_m\Delta U^2 W_e/z_i,$$

where C_m is a coefficient that is inversely related to the normalized inversion layer thickness $\Delta h/z_i$. The TKE equation is closed to permit calculation of W_e by assigning an expression for the dissipation rate based on dimensional analysis. For example,

$$\epsilon = C_D W_m^2 \omega_B,$$

where C_D is another coefficient and ω_B is the Brunt–Väisälä frequency. Tennekes and Driedonks offer several other candidate expressions, alert the reader to the arbitrary nature of these expressions and identify the dissipation term as a major problem.

In this paper a slightly different approach will be taken. The shear production term will be evaluated (Section 3) using WLs inversion layer integral formalism which has proved quite successful with the scalar variance budgets. The WL expressions are modified (Section 2) based on comparison with aircraft data. A completely separate closure relation for the dissipation term is obtained from the vertical velocity variance (σ_w^2) budget equation (Section 4). Since this introduces another unknown (namely, σ_w), Deardorff's (1980) empirical relation between W_e and σ_w at the inversion is used to complete the solution. The rationale for this approach is the perceived intimate connection between entrainment and vertical velocity turbulence.

2. Background

a. Inversion structure parameters

The structure function parameters for temperature C_T^2 and specific humidity C_Q^2, are to be evaluated in the inversion region by averaging between heights $z = h_0$ and $z = h_2$ (see Fig. 1). The theory is developed in complete detail by WL so only background material will be presented here. One major departure will be the treatment of entrainment velocity W_e. Wyngaard and LeMone make explicit substitutions for W_e based on convective PBL theory, whereas in this paper W_e must be carried as an unknown variable in anticipation of a dependence on wind shear.

The height h_0 is defined as the top of the mixed layer where $\overline{w\theta_v} = 0$. At h_2 both fluxes and flux divergences are equal to zero. The inversion is assigned the height z_i. The interfacial layer average of a turbulence variable $\psi(z)$ is defined

$$\langle\psi(z)\rangle = \Delta h^{-1}\int_0^2 \psi(z)dz, \tag{2}$$

where $\Delta h = h_2 - h_0$ and the 0, 2 on the integral denotes h_0, h_2. The average structure functions are related to their respective dissipation rates by the Corrsin equation

$$\langle C_T^2\rangle = 1.6\langle\epsilon\rangle^{-1/3}\langle\chi_\theta\rangle, \tag{3a}$$

$$\langle C_Q^2\rangle = 1.6\langle\epsilon\rangle^{-1/3}\langle\chi_Q\rangle, \tag{3b}$$

where ϵ is the rate of dissipation of turbulent kinetic energy, and χ_θ and χ_Q are the scalar dissipation rates. The coefficient 1.6 implies χ_θ is the rate of dissipation of temperature variance θ^2 rather than $\theta^2/2$ and is assumed to apply to χ_Q.

b. Evaluation of $\langle\chi\rangle$

For the purpose of illustration, the discussion will be confined to the absolute humidity (Q). The dissipation rate is calculated from the scalar variance budget equation which is integrated from h_0 to h_2 as in (2),

$$\langle\chi_Q\rangle = -\langle D_Q\rangle - \langle T_Q\rangle - \langle P_Q\rangle, \tag{4}$$

where D_Q is the divergence term, T_Q transport and P_Q gradient production. Assuming "quasi-steady" conditions, WL use aircraft and balloon data to show that $\langle D_Q\rangle$ and $\langle T_Q\rangle$ are negligible compared to $\langle P_Q\rangle$; therefore

$$\langle\chi_Q\rangle \approx -\langle P_Q\rangle. \tag{5}$$

At this point the generalized inversion structure model (Deardorff, 1979) is introduced where a function $f(z)$

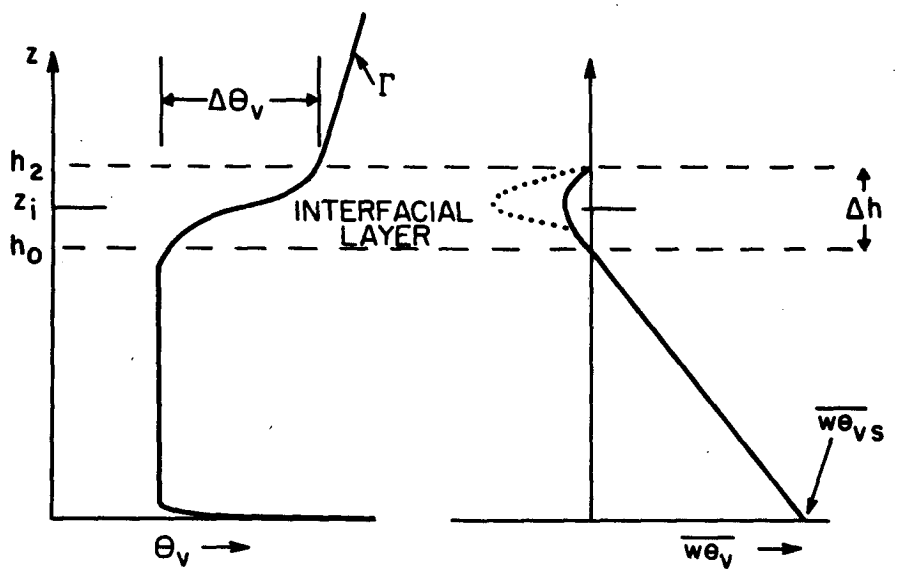

FIG. 1. Schematic diagram of the convective boundary layer with its interfacial layer. The top of the mixed layer is h_0, the top of the boundary layer is h_2 and z_i is the inversion height. Dotted line on the buoyancy flux profile indicates the local enhancement due to shear production of turbulent kinetic energy.

describes the shape of the Q profile in the inversion region (assumed to be the same for Q and θ_v) with ΔQ the jump in Q across the inversion.

With a bit of manipulation, WL evaluate the integral in (5). Their results for χ_Q and χ_θ can be expressed

$$\langle X_Q \rangle = \frac{7(\Delta Q)^2 \Gamma W_e}{6\Delta\theta_v}, \tag{6a}$$

$$\langle X_{\theta_v} \rangle = \frac{\Delta\theta_v \Gamma W_e}{6}, \tag{6b}$$

where Γ is the lapse rate of θ_v above the inversion and the entrainment velocity is defined at $z = z_i$.

Their solution involved usage of the bulk stability parameters R and S given by

$$R = g\Delta\theta_v z_i/(W_*^2 T), \tag{7a}$$

$$S = g\Gamma z_i^2/(W_*^2 T), \tag{7b}$$

where W_* is the convective scaling velocity defined in terms of the surface buoyancy flux

$$W_*^3 = g\overline{w\theta_{vs}} z_i/T. \tag{8}$$

In the convective case evaluated by WL, the structure functions are obtained from (3) assuming that the average value of the rate of dissipation of TKE is one half the convective limit

$$\langle \epsilon \rangle = \langle \epsilon \rangle_c = 0.5\epsilon_c = 0.2 W_*^3/z_i \tag{9}$$

and by explicitly substituting the quasi-equilibrium entrainment rate W_{eq} from Deardorff (1979)

$$W_{eq} = W_*/S. \tag{10}$$

The calculation of the refractive index structure parameter requires correction factors (see WL) to convert the virtual temperature forms given by (6b) to the potential temperature variables of (1).

c. Comparison with data

Data from AMTEX, GATE and Puerto Rico were used by WL to verify their structure parameter expressions. Dubosclard (1982) has also published some comparisons with acoustic sounder measurements. In the interest of comparing these with an independent data set, cloud-free, unstable boundary layer profiles were abstracted from previous aircraft measurements available to the author (Fairall *et al.*, 1980; Markson *et al.*, 1981). Paired microthermal temperature sensors (C_T^2), a hot wire (ϵ) and a Lyman-alpha fast response hygrometer (C_Q^2) were used. Details about the data and analysis techniques can be found in Fairall (1982). Three overwater [near Monterey, CA (MY), near Panama City, FL (PC) and near the Bahamas (BH)] and one overland [White Sands, NM (WS)] field deployments yielded 22 usable profiles under an impressive variety of boundary layer conditions. Relevant parameters for these profiles are summarized in Table 1 (note that the average brackets $\langle\ \rangle$ indicate one half the peak value for these data). The surface layer scaling parameters u_* (velocity), T_* (temperature), q_* (mixing ratio), and L (Monin–Obukhov length) follow the usual definitions (Wyngaard, 1973).

A comparison with the expressions developed by WL is given in Fig. 2a. The apparent dependence of

TABLE 1. Boundary layer parameters for aircraft profiles.

Number	Site	u_* (m s^{-1})	T_* (K)	q_* (g kg^{-1})	z_i (m)	$\Delta\theta_v$ (K)	ΔQ (g m^{-3})	Γ (K km^{-1})	$-L$ (m)	W_* (m s^{-1})	R/S	$10^3\langle C_T^2\rangle$ (K^2 m$^{-2/3}$)	$10^3\langle C_Q^2\rangle$ [(g m^{-3})^2 m$^{-2/3}$]	$10\langle\epsilon\rangle^{1/3}$ (m$^{2/3}$ s^{-1})
1	PC	0.40	−0.082	−0.16	850	1	−6.5	5.5	125	1.1	0.32	1.0		0.63
2	PC	0.23	−0.095	−0.16	910	0.5	−2.3	5.3	50	0.93	0.10	2.8		0.96
3	PC	0.24	−0.14	−0.18	230	4	−0.5	4.6	30	0.67	3.7	2.5		1.0
4	PC	0.38	−0.35	0	910	6	−1	10	35	1.6	0.67	6.		0.74
5	PC	0.32	−0.49	−0.49	750	0.3	−1	11	13	1.7	0.36	5.5		0.73
6	PC	0.34	−0.48	−0.48	850	3	−1.3	11	17	1.7	0.32	2.8		0.84
7	PC	0.34	−0.49	−0.50	1100	3	−3	17.5	15	1.9	0.16	4.5		0.71
8	PC	0.28	−0.44	−0.43	700	3	−1	9.5	25	1.5	0.46	22		1.1
9	PC	0.19	−0.21	−0.47	600	1.5	−0.2	10	10	1.0	0.35	3		0.63
10	PC	0.17	−0.20	−0.42	500	0.5	−2	11	9	0.92	0.10	1.7		1.0
11	WS	0.47	−0.42	0	1100	1.5	−0.25	3	45	1.9	0.44	4.6		1.1
12	WS	0.47	−0.42	0	1900	1.6	−2.5	3.3	45	2.3	0.24	1.5	2	1.1
13	MY	0.28	−0.078	−0.11	360	6.5	−4.5	9	70	0.65	2.2	1.3	1	1.3
14	MY	0.21	−0.085	−0.11	360	11	−5.2	10	40	0.60	3.7	0.5	5	0.46
15	MY	0.30	−0.075	−0.12	460	9	−5.2	15	120	0.70	1.5	5	12	0.87
16	MY	0.30	−0.075	−0.12	540	9	−5	15	120	0.75	1.6	1.4	0.8	0.46
17	MY	0.41	−0.040	−0.05	230	7	52	9	300	0.50	3.7	0.8	16	0.63
18	BH	0.15	−0.30	−0.27	500	1	−2.5	5	10	0.79	0.4	3.4	1.6	0.40
19	BH	0.23	−0.17	−0.27	900	2.5	−8.5	6.3	22	1.1	0.45	1.4	8	0.84
20	BH	0.20	−0.16	−0.26	1500	3.5	−9	5.5	17	1.25	0.42		35	0.55
21	BH	0.20	−0.16	−0.26	1500	3.5	−9	5.5	17	1.25	0.42		8	1.1
22	BH	0.14	−0.14	−0.25	1100	1	−4.5	6.3	10	0.95	0.14		27	0.48

the ratio of measured and calculated values on the value of R/S suggests that the more traditional convective entrainment parameterization (Stull, 1976)

$$W_{ec} = 0.2W_*/R = 0.2W_{eq}S/R \tag{11}$$

is a better choice. This is somewhat reassuring since (11) has proven successful for the classic convective boundary layer. The comparison was further improved (Fig. 2b) by using the mixed layer scaling velocity W_m

$$W_m^3 = W_*^3 + 8u_*^3, \tag{12}$$

as suggested by Tennekes and Driedonks (1981), so that

$$W_{ec} = 0.2W_m/R, \tag{13a}$$

$$R = g\Delta\theta_v z_i/(W_m^2 T), \tag{13b}$$

$$S = g\Gamma z_i^2/(W_m^2 T), \tag{13c}$$

$$\langle\epsilon\rangle_c = 0.2W_m^3/z_i. \tag{13d}$$

The scaling velocity W_m^2 is used for the remainder of this paper.

3. Dissipation of TKE

The rate of dissipation of TKE, ϵ, is of use both through its effect on the structure functions (3) and as a component in the vertical velocity variance budget (to be discussed in Section 4). The influence of entrainment and inversion layer shear production on ϵ is evaluated by applying the WL model approach to the TKE budget equation

$$\frac{D\bar{e}}{Dt} + \overline{uw}\frac{\partial U}{\partial z} + \overline{vw}\frac{\partial V}{\partial z} + \frac{\partial}{\partial z}(\overline{we}) + \rho^{-1}\frac{\partial}{\partial z}(\overline{wp}) - \frac{g}{T}\overline{\theta_v w} = -\epsilon, \tag{14}$$

where $e = \frac{1}{2}(u^2 + v^2 + w^2)$, p is the fluctuating kinematic pressure and the other notation is standard (Lenschow *et al.*, 1980). The inversion layer averages are formed similarly to (4)

$$-\langle D_e\rangle - \langle P_e\rangle - \langle T_e\rangle - \langle I_e\rangle - \langle B_e\rangle = \langle\epsilon\rangle, \tag{15}$$

where D_e denotes the total time derivative, $-P_e$ the shear production, T_e the transport, I_e the pressure transport (usually obtained as an imbalance or residual of the other terms), and B_e the buoyant destruction.

Assuming that the wind profile has the same inversion shape function as the scalar profile, then by analogy with the water vapor expression (6a)

$$-\langle P_e\rangle = \frac{7(\Delta S_h)^2\Gamma W_e}{12\Delta\theta_v}, \tag{16}$$

where $(\Delta S_h)^2 = (\Delta U)^2 + (\Delta V)^2$ and the extra factor of one half is due to the definition of TKE as one half the sum of the velocity variances. The assumption

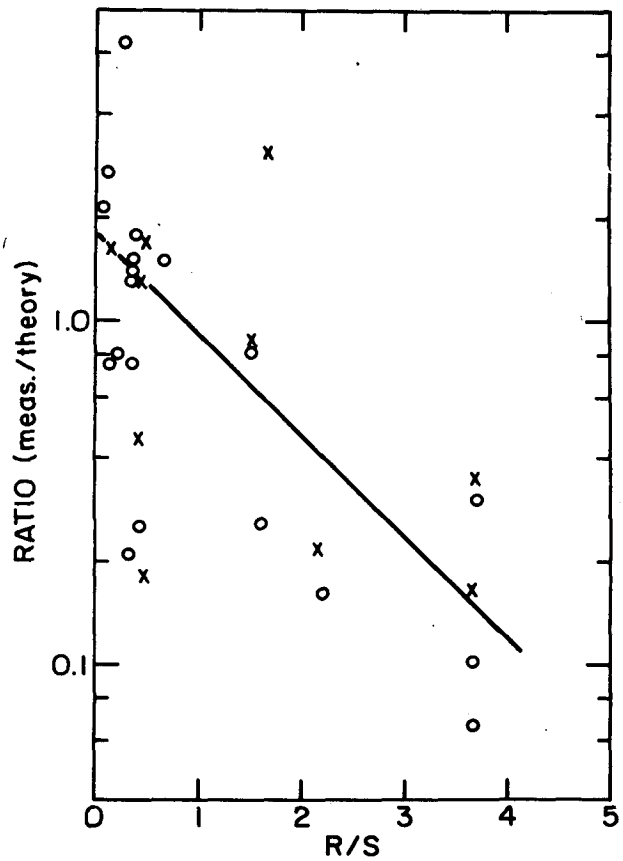

FIG. 2a. The ratio of aircraft structure function measurements C_T^2 (circles) and C_Q^2 (crosses) to the Wyngaard-LeMone theory predictions as a function of R/S.

of inversion, wind and scalar profile similarity is essentially forced by the difficulties associated with making high vertical resolution wind profile measurements. The assumption must fail in those shear driven layers characterized by a constant gradient Richardson number (e.g., $\sim$¼) since this condition implies the velocity gradient squared is proportional to the virtual potential temperature gradient. The buoyant term is given by

$$-\langle B_e\rangle = -\frac{1}{2}(g/T)W_e\Delta\theta_v. \tag{17}$$

The time derivative and transport terms are again assumed negligible (this is also consistent with the measurements of Lenschow *et al.*, 1980). In the limit of negligible shear production (which shall be referred to as the convective limit), the imbalance is

$$\langle I_e\rangle = \frac{3}{2}\langle\epsilon\rangle_c. \tag{18}$$

Measurements obtained by Brost *et al.* (1982) under conditions of very strong wind shear (their case 17-2; see Fig. 3a) indicates that the imbalance term does not scale with $(\Delta S_h)^2$ or W_e (since this paper will be cited often, it is hereafter referred to as BWL). This is consistent with the divergence term scaling as $C_F W_m^3/z_i$ (where C_F is an empirical coefficient) as suggested by Zilitinkevich (1975) and discussed at some length by Tennekes and Driedonks (1981). The final result (assuming $\langle I_e\rangle = \langle I_e\rangle_c$) is

$$\langle\epsilon\rangle = \frac{3}{2}\langle\epsilon\rangle_c + \frac{7(\Delta S_h)^2\Gamma W_e}{12\Delta\theta_v} - \frac{1}{2}(g/T)W_e\Delta\theta_v, \tag{19}$$

which can be written

$$\langle\epsilon\rangle = \langle\epsilon\rangle_c\left[\frac{3}{2} + \frac{1}{2}(R_f^{-1} - 1)X\right], \tag{20}$$

where R_f is the flux Richardson number for the interfacial layer

$$R_f^{-1} = \frac{7(\Delta S_h)^2\Gamma}{6(g/T)(\Delta\theta_v)^2}, \tag{21}$$

and X is a dimensionless entrainment velocity (equal to one in the convective limit),

$$X = 5RW_e/W_m, = W_e/W_{ec}, \tag{22}$$

where R is given by (13b).

The results summarized in (20) imply that the mixed layer profiles of the terms of the TKE budget

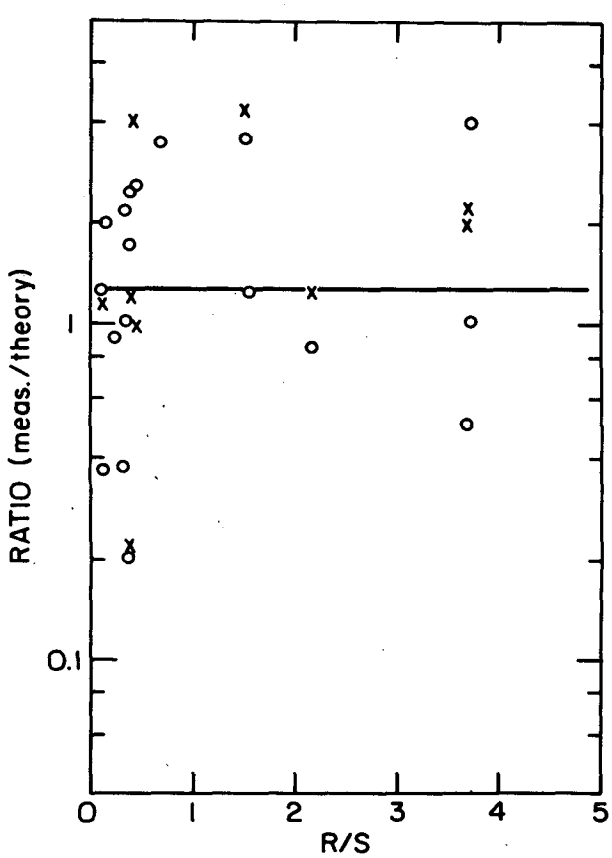

FIG. 2b. As in Fig. 2a but using Eq. (21) for entrainment and Eq. (22) for the boundary layer scaling velocity.

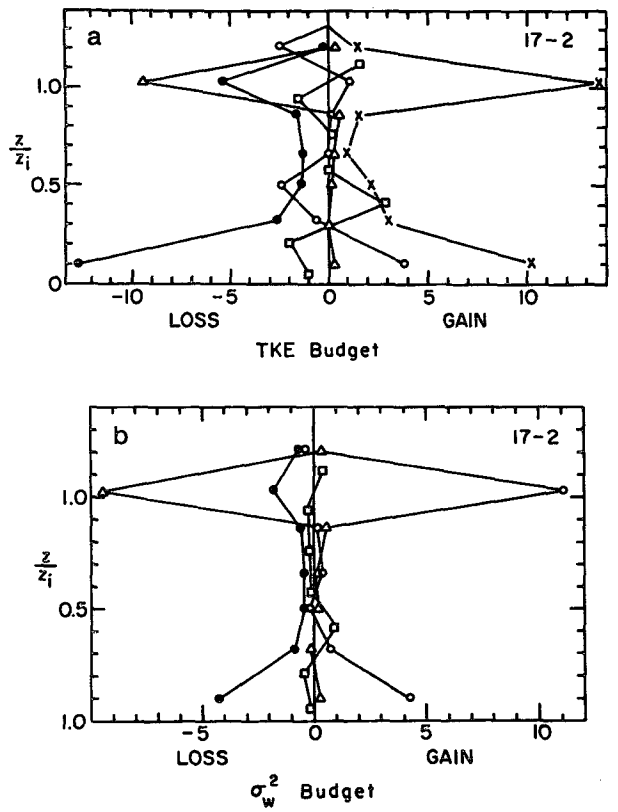

FIG. 3. (a) Normalized terms of the turbulent kinetic energy budget from Brost *et al.* (1982) field study case 17-2. The inversion wind shear was approximately 10 m s^{-1}. All budget terms are multiplied by kz_i/u_*^3 to make them nondimensional. The terms are: dissipation ϵ (solid circles); shear production $[-\overline{uw}(\partial U/\partial z) - \overline{vw}(\partial V/\partial z)]$ (crosses); buoyant production $(g/T_0)\overline{w\theta_v}$ (open triangles); turbulent transport $-(\partial\overline{we}/\partial z)$ (open squares); and the imbalance term I required for the budget to balance (open circles).

(b) As in (a) but for the one-half vertical velocity variance budget. All terms are nondimensionalized by kz_i/u_*^3. Terms are: dissipation $\epsilon/3$ (solid circles); buoyant production $(g/T_0)\overline{w\theta_v}$ (open triangles); turbulent transport $-(\partial/\partial z)(\overline{w^3}/2)$ (open squares); and the imbalance term required for budget to balance (open circles).

are relatively unchanged by inversion wind shear. The additional TKE produced by the shear is either dissipated or buoyantly destroyed in the interfacial region (thus the dotted line depicted in the buoyancy flux profile in Fig. 1) while the pressure imbalance term remains relatively unaffected. This view is qualitatively supported by case 17-2 reported by BWL (Fig. 3a). The presence of cloud top radiative cooling precludes the use of this data for quantitative evaluation of (20) although it is of interest to observe that $R_f^{-1} = 1.4$ for this case.

4. Vertical velocity variance

a. Deardorff parameterization

The vertical velocity variance ($\overline{w^2}$) is an important parameter in the entrainment process. Deardorff (1980) produced a relationship between W_e and the value of the variance at the inversion ($\overline{w^2} = \sigma_{wi}^2$)

$$\frac{W_e}{\sigma_{wi}} = \frac{C_r \Delta R}{\Delta\theta_v \sigma_{wi}} + \text{fcn}(R_\sigma), \tag{23}$$

where ΔR is the radiation jump across the inversion, R_σ is a Richardson number

$$R_\sigma = (g/T)\Delta\theta_v Z_i/\sigma_{wi}^2 \tag{24}$$

and fcn is an empirical function approximately given by

$$\text{fcn}(R_\sigma) = AR_\sigma^{-3/2}, \tag{25}$$

where $A = 100$. Deardorff's (1980) result is based on three-dimensional numerical model (subgrid closure) simulations of clear (three cases) and stratocumulus capped (ten cases) mixed layers. The expression was found by BWL to give very good agreement with their data using the coefficient $C_r = 0.75$. For the cloud-free case ($\Delta R = 0$ so the value of C_r is unimportant), (13) can be written

$$\frac{\sigma_{wi}^2}{W_m^2} = \frac{R^{1/4}}{(5A)^{1/2}} X^{1/2}, \tag{26}$$

which in the convective limit ($X = 1$) implies

$$\frac{\langle\sigma_w^2\rangle_c}{W_m^2} = \frac{R^{1/4}}{2(5A)^{1/2}}, \tag{27a}$$

$$\langle\sigma_w^2\rangle = \langle\sigma_w^2\rangle_c X^{1/2}. \tag{27b}$$

b. Interfacial average

The average velocity variance in the interfacial region, $\langle\sigma_w^2\rangle$, can be evaluated in a like manner to the dissipation rate development in Section 3. The beginning point for this process is the budget equation (see BWL for details on the individual terms)

$$-\langle D_w\rangle - \langle T_w\rangle - \langle I_s\rangle - \langle I_t\rangle - \langle B_w\rangle = \tfrac{1}{3}\langle\epsilon\rangle, \tag{28}$$

where D_w is the total time derivative of $\overline{w^2}/2$, T_w the turbulent transport term, I_s the pressure scrambling term, I_t the pressure transport term and B_w the buoyant destruction term. The time derivative, pressure transport and turbulent transport terms are assumed negligible (see the discussion by BWL). The vertical velocity variance data set, from BWL case 17-2, is shown in Fig. 3b to illustrate the dominance of the remaining terms at the inversion,

$$-\langle I_s\rangle - \langle B_w\rangle - \tfrac{1}{3}\langle\epsilon\rangle = 0. \tag{29}$$

The pressure scrambling term, which is approximated as the sum of a Rotta return to isotropy term and a "rapid" term (Launder, 1975), is expressed as

$$-2I_s = c_1\epsilon/3 - c_1\epsilon\sigma_w^2/q^2 + \tfrac{4}{3}c_2 B_w \tag{30}$$

for $q^2 = 2e$ (q is now the turbulence velocity scale). The two terms c_1 and c_2 are "constants" which BWL have interrelated using surface layer scaling arguments

$$c_1 \approx 14(1 - c_2). \tag{31}$$

It is not clear that (31) is relevant in the inversion region. Brost, Wyngaard and Lenschow note that second order closure modelers typically use values of c_1 between three and nine. Combining (17), (29) and (30) yields

$$c_1\langle\epsilon\sigma_w^2/q^2\rangle = 2(c_1/2 - 1)\langle\epsilon\rangle/3 - \frac{g}{T}\left(1 - \frac{2}{3}c_2\right)W_e\Delta\theta_v. \tag{32}$$

The evaluation of the left-hand side of (32) requires some handwaving which, if not rigorous, should at least be plausible. Since the ratio σ_w^2/q^2 should be roughly constant in the inversion region, one can approximate the average products by

$$\langle\epsilon\sigma_w^2/q^2\rangle \approx \langle\epsilon\rangle\langle\sigma_w^2/q^2\rangle \approx \langle\epsilon\rangle\langle\sigma_w^2\rangle/\langle q^2\rangle. \tag{33}$$

Thus, (32) can be written

$$\frac{\langle\sigma_w^2\rangle}{W_m^2} = \frac{W_m\langle q^2\rangle}{5c_1\langle\epsilon\rangle z_i}\left\{(c_1/2 - 1)\left[1 + \frac{1}{3}(R_f^{-1} - 1)X\right] - (1 - \frac{2}{3}c_2)X\right\}. \tag{34}$$

In order to eliminate $\langle q^2\rangle$ we must argue that $\langle q^2\rangle$ and $\langle\epsilon\rangle$ have approximately the same scaling dependence on wind shear so their ratio can be determined in the convective limit ($X = 1$, $R_f^{-1} = 0$)

$$\frac{\langle\sigma_w^2\rangle_c}{W_m^2} = \frac{W_m\langle q^2\rangle}{5c_1\langle\epsilon\rangle z_i}\frac{(c_1 + 2c_2 - 5)}{3}. \tag{35}$$

To justify this assumption, consider the classical relation $\epsilon = C_\epsilon q^3/l_\epsilon$ where C_ϵ is a constant and l_ϵ an appropriate length scale. Deardorff's (1974) three-dimensional simulations showed l_ϵ decreasing in the inversion. In such stable layers, the length scale is a function of the Brunt–Väisälä frequency (Therry and LaCarrere, 1983), $l_\epsilon \sim q/\omega_B$. Thus, $\langle\epsilon\rangle/\langle q^2\rangle$ is independent of wind shear and entrainment. The final result is

$$\langle\sigma_w^2\rangle = \langle\sigma_w^2\rangle_c[1 + rR_f^{-1} + (rR_f^{-1} - s)(X - 1)], \tag{36}$$

where

$$r = \frac{c_1 - 2}{2(c_1 + 2c_2 - 5)}, \tag{37a}$$

$$s = \frac{c_1 - 4c_2 + 4}{2(c_1 + 2c_2 - 5)}, \tag{37b}$$

$$\frac{\langle\sigma_w^2\rangle_c}{\langle q^2\rangle_c} = (c_1 + 2c_2 - 5)/(3c_1). \tag{37c}$$

Note that (31) and (37c) imply $c_1 > 3.5$ while $c_1 = 11$ gives $\langle\sigma_w^2\rangle_c/\langle q^2\rangle_c \approx 0.18$ which is a typical observed value.

5. Entrainment

The application of the WL formulation to the budget of TKE and vertical velocity variance led to parameterizations in terms of the entrainment rate (at this point still an unknown). The "closure" for this system of equations is Deardorff's empirical expression (27b) which is equated to (36)

$$X^{1/2} = 1 + rR_f^{-1} + (rR_f^{-1} - s)(X - 1), \tag{38}$$

and can be solved as a quadratic equation. A simple approximation (with more than sufficient accuracy considering the number of simplifications necessary to obtain Eq. 38) is

$$Y = X - 1 = \frac{rR_f^{-1}(2 + rR_f^{-1})}{1 + 2(1 + rR_f^{-1})(s - rR_f^{-1})}. \tag{39}$$

Note that (38) becomes singular at

$$R_f^{-1} = s/r = \frac{c_1 - 4c_2 + 4}{c_1 - 2}. \tag{40}$$

The implication of this behavior is that transition to inversion *shear driven* entrainment occurs if R_f^{-1} exceeds s/r.

The effect of the entrainment enhancement on the refractive index structure parameter is a straightforward calculation from (1), (3) and (6), i.e.,

$$\langle C_N^2\rangle/\langle C_N^2\rangle_c = (\langle\epsilon\rangle/\langle\epsilon\rangle_c)^{-1/3}X \tag{41}$$

or

$$\langle C_N^2\rangle/\langle C_N^2\rangle_c = \frac{1 + Y}{[1 + R_f^{-1}/2 + \frac{1}{2}(R_f^{-1} - 1)Y]^{1/3}}. \tag{42}$$

An illustration of the results of (39) and (42) is given in Fig. 4 for a choice of constants ($c_1 = 11$) such that the singularity occurs for $R_f^{-1} \approx 2$. Note that in this case the effects on C_N^2 becomes significant (on the order of the factor of 2 accuracy of the WL model) when $W_e/W_{ec} \approx 3$ and $R_f^{-1} \approx 1.5$.

6. Wind shear assessment

a. Mixed layer winds

The two horizontal wind components can be treated in a conventional mixed layer formulation (Tennekes and Driedonks, 1981; Garratt *et al.*, 1982; Wyngaard, 1983).

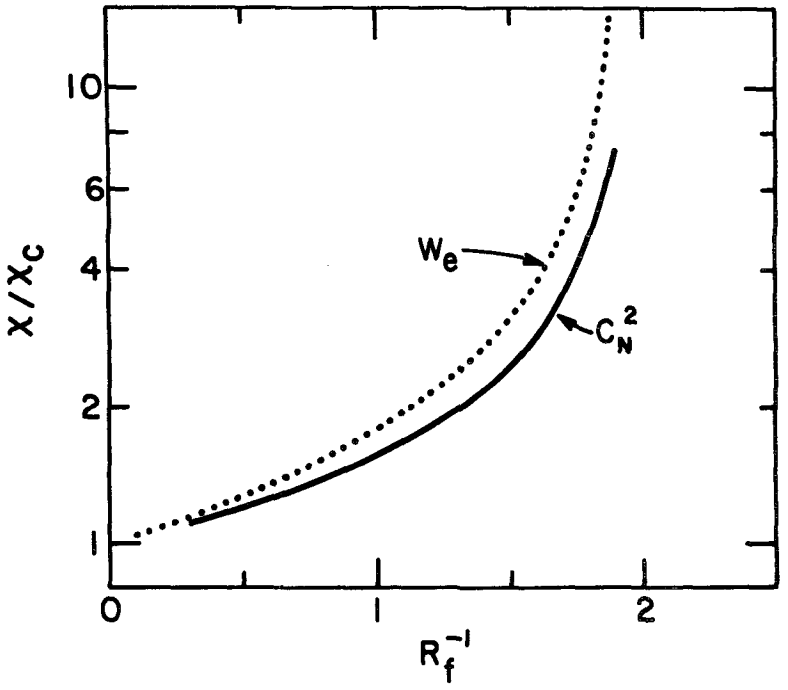

FIG. 4. Values of entrainment (dotted line) and refractive index structure parameter (solid line) normalized by their convective limits (no shear) as a function of R_f^{-1} for $s/r \sim 2$.

$$\frac{D\hat{U}}{Dt} = f\hat{V} - \frac{1}{\rho}\partial P/\partial x - \frac{g}{T}\left(\Delta\theta_v \partial z_i/\partial x - \frac{1}{2} z_i \partial\theta_v/\partial x\right) + \frac{W_e}{z_i}(U_g - \hat{U}) - c_d\hat{U}(\hat{U}^2 + \hat{V}^2)^{1/2}/z_i, \quad (43a)$$

$$\frac{D\hat{V}}{Dt} = -f\hat{U} - \frac{1}{\rho}\partial P/\partial y - \frac{g}{T}\left(\Delta\theta_v \partial z_i/\partial y - \frac{1}{2} z_i \partial\theta_v/\partial y\right) + \frac{W_e}{z_i}(V_g - \hat{V}) - c_d\hat{V}(\hat{U}^2 + \hat{V}^2)^{1/2}/z_i, \quad (43b)$$

where c_d is the mixed layer drag coefficient and the caret indicates a mixed layer average. Consider the simplification where the winds above the inversion are identified with the horizontal pressure gradients (which shall be called the geostrophic component)

$$U_g = -\frac{1}{f\rho}\partial P/\partial y, \quad (44a)$$

$$V_g = \frac{1}{f\rho}\partial P/\partial x, \quad (44b)$$

and the horizontal gradients of mixed layer temperature and depth are termed "baroclinic" contributions

$$\Delta U_g = \frac{1}{f}\frac{g}{T}\left(\Delta\theta_v \partial z_i/\partial y - \frac{1}{2} z_i \partial\theta_v/\partial y\right), \quad (45a)$$

$$\Delta V_g = -\frac{1}{f}\frac{g}{T}\left(\Delta\theta_v \partial z_i/\partial x - \frac{1}{2} z_i \partial\theta_v/\partial x\right), \quad (45b)$$

where

$$\hat{U}_g = U_g - \Delta U_g, \quad (46a)$$

$$\hat{V}_g = V_g - \Delta V_g, \quad (46b)$$

such that a negative value of ΔU_g implies accelerated boundary layer flow. If the inversion layer shears are defined as

$$\Delta U = U_g - \hat{U}, \quad (47a)$$

$$\Delta V = V_g - \hat{V}, \quad (47b)$$

then (43) can be written

$$\frac{1}{f}\frac{D\hat{U}}{Dt} = -\Delta V + \Delta V_g + \frac{W_e}{fz_i}\Delta U - \frac{c_d\hat{U}(\hat{U}^2 + \hat{V}^2)^{1/2}}{fz_i}, \quad (48a)$$

$$\frac{1}{f}\frac{D\hat{V}}{Dt} = \Delta U - \Delta U_g + \frac{W_e}{fz_i}\Delta V - \frac{c_d\hat{V}(\hat{U}^2 + \hat{V}^2)^{1/2}}{fz_i}. \quad (48b)$$

b. Barotropic equilibrium

Although (48) describes the dynamic behavior of the mixed layer winds, a case study of all relevant variations of initial conditions would be lengthy indeed. Since we are particularly interested in assessing the probable influence of wind shear, it is reasonable to deal with the equilibrium case on the grounds that it is an estimate of the average expected conditions (note that this is not to say the mixed layer wind is expected to be in equilibrium). Clearly a large baroclinic contribution can be specified (ΔU_g large) and a significant wind shear will result in the equilibrium condition, but this is probably unenlightening given the tendency for feedback to development between the pressure gradient, temperature gradient and the slope of the inversion (Overland *et al.*, 1983). Suffice it to say that wind shear is likely to develop in coastal regions, the marginal ice zone, the boundary of the Gulf Stream and other areas characterized by strong horizontal variability.

The simplest case of interest is the horizontally homogeneous, equilibrium condition which might characterize the open ocean under reasonably steady synoptic forcing. For simplicity, the coordinates are defined such that $\hat{V} = 0$ (therefore $\Delta V = V_g$) which leads to the following equilibrium equation:

$$\Delta V = \frac{W_e}{fz_i}\Delta U - \frac{c_d}{fz_i}(U_g - \Delta U)^2, \tag{49a}$$

$$\Delta U = -\frac{W_e}{fz_i}\Delta V. \tag{49b}$$

For reasonably small wind shears a simple solution to these equations is

$$\Delta V = \frac{-c_d U_g^2}{fz_i[1 + (2c_d U_g + W_e)W_e/(fz_i)^2]}. \tag{50}$$

c. Case studies

Given a synoptic wind forcing S_g,

$$S_g^2 = U_g^2 + V_g^2, \tag{51}$$

which is assumed to be the ambient wind speed at the top of the boundary layer, then (39), (49b) and (50) can be solved numerically to yield the equilibrium wind shear and entrainment rate subject to the specification of other scaling parameters. For this study, only the nearly neutral marine boundary layer will be considered. The drag coefficient is assigned the value $c_d = 1.3 \times 10^{-3}$ which is consistent with the AMTEX values obtained by Garratt *et al.*, (1982). The boundary layer scaling velocity is

$$W_m^3 = W_*^3 + 8c_d^{3/2}(U_g - \Delta U)^3, \tag{52}$$

so W_* is another parameter that must be specified. The flux Richardson number obeys the relation

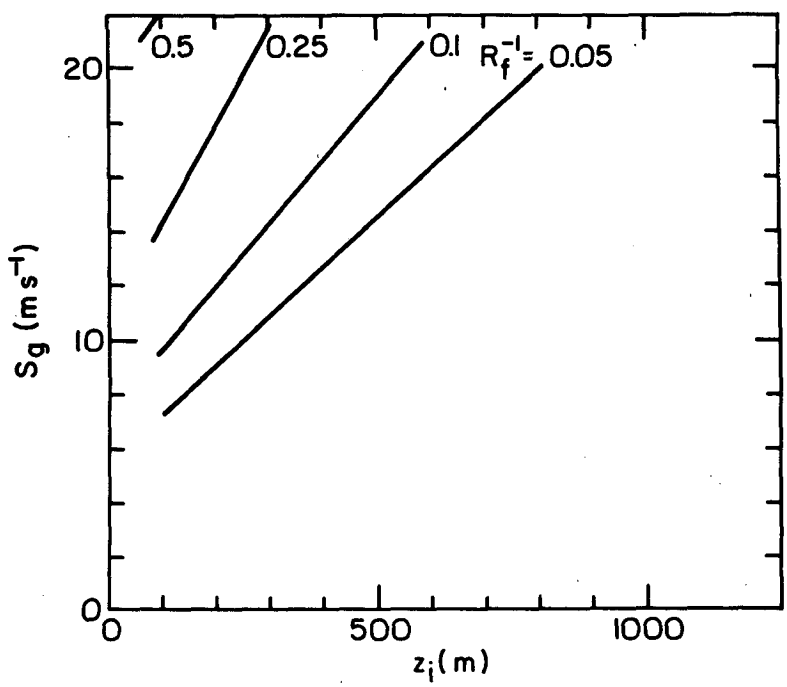

FIG. 5a. Contours of R_f^{-1} under equilibrium conditions as a function of geostropic forcing (S_g) and inversion height (z_i) for $W_* = 1.0$, $R = 100$ and $R/S = 3.3$.

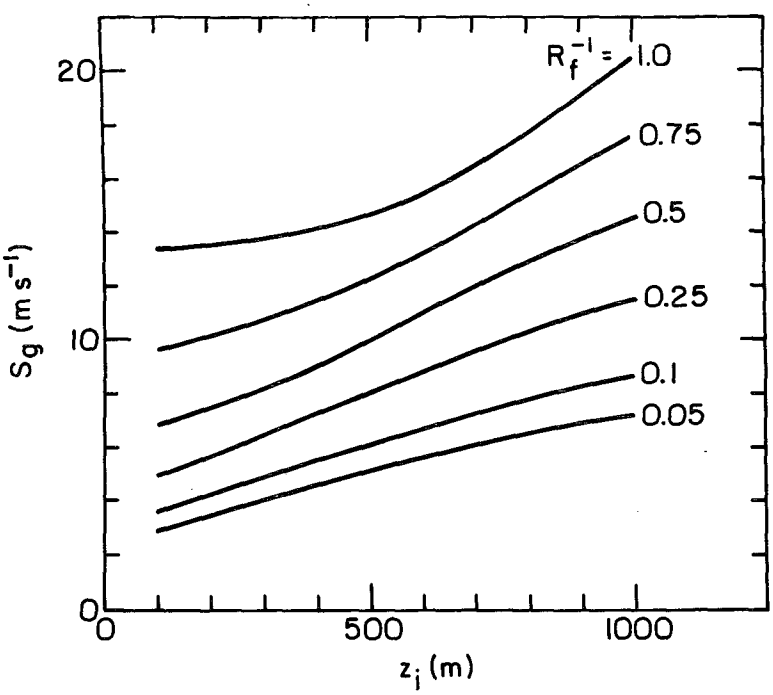

FIG. 5b. As in Fig. 5a but for $R = 30$ and $R/S = 0.3$.

$$R_f = \frac{6R(R/S)}{7}\frac{W_m^2}{(\Delta S_h)^2}, \quad (53)$$

and f is assigned a value of 10^{-4}.

The equilibrium condition has been displayed as contour plots with S_g and z_i as the primary axes. In Fig. 5, contours of R_f^{-1} are plotted for specified values of s, r, W_*, R and R/S. Small values of R_f^{-1} imply negligible wind shear is present under equilibrium

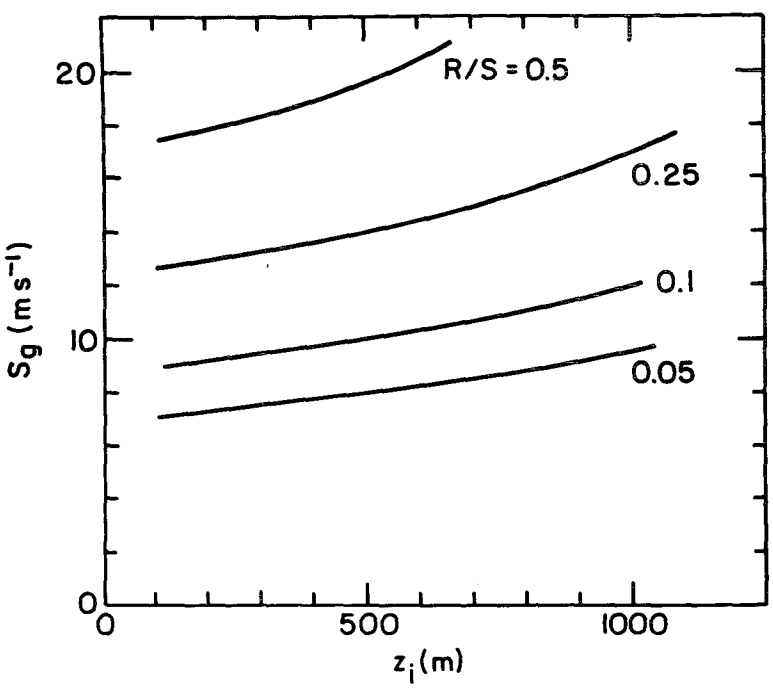

FIG. 6a. Contours of R/S under equilibrium conditions for a factor of 2 increase in C_N^2 due to wind shear as a function of S_g and z_i for $W_* = 1.0$ and $R = 10$.

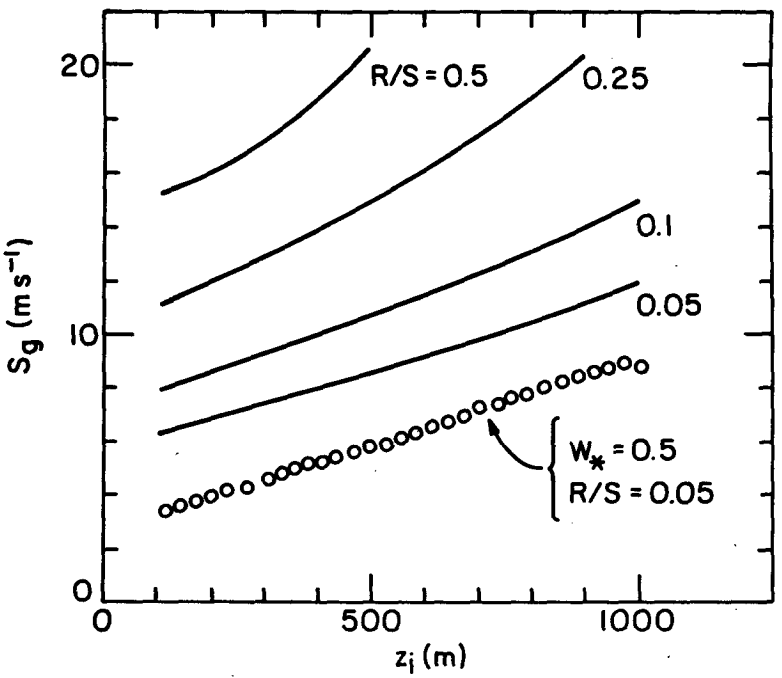

FIG. 6b. As in Fig. 6a but for $R = 30$.

conditions. The same values of s and r used for Fig. 4 have been used for all of the remaining graphs; therefore, a value of $R_f^{-1} = 1.5$ corresponds to the threshold of significant wind shear effects on C_N^2. Likely C_N^2 effects can be explored by specifying $R_f^{-1} = 1.5$ and plotting contours (Fig. 6) of the resultant values of R/S from (53) for specified values of R. From these results it appears that small values of R/S are more likely to produce substantial wind shear enhancements of C_N^2. The effect of buoyant convection (W_*) is illustrated in Fig. 7 where larger amounts of geostrophic forcing are required to produce significant enhancement in the presence of strong convective entrainment. Examples of wind

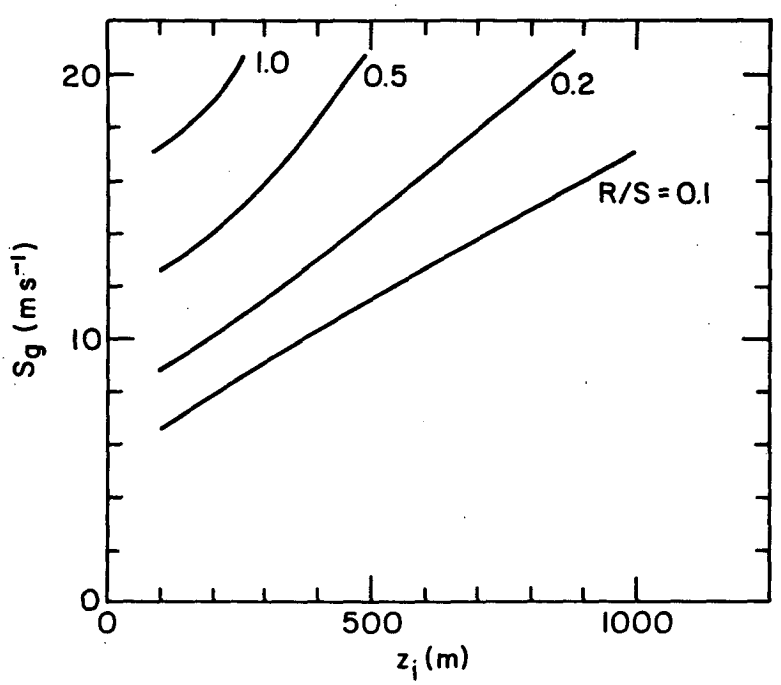

FIG. 6c. As in Fig. 6a but for $R = 100$.

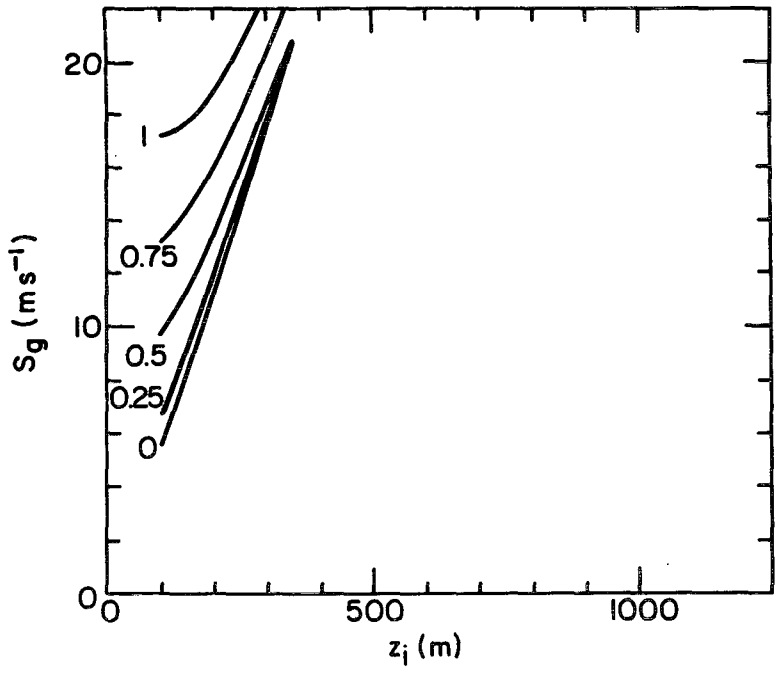

FIG. 7. Contours of W_* under equilibrium conditions for a factor of 2 increase in C_N^2 due to wind shear as a function of S_g and z_i with $R = 100$ and $R/S = 1$.

shear components in equilibrium at $R/S = 0.2$, $W_* = 1$ m s^{-1} and $R_f^{-1} = 1.5$ are shown in Fig. 8.

7. Conclusions

A simple model of the enhancement of the entrainment rate of a convective boundary layer by interfacial shear production of turbulent kinetic energy has been developed using techniques similar to that of Wyngaard and LeMone (1980). First, some minor modifications to their model were made since better agreement with a set of aircraft structure function parameter data was obtained using the convective entrainment formulation from Stull (1976) and the boundary layer

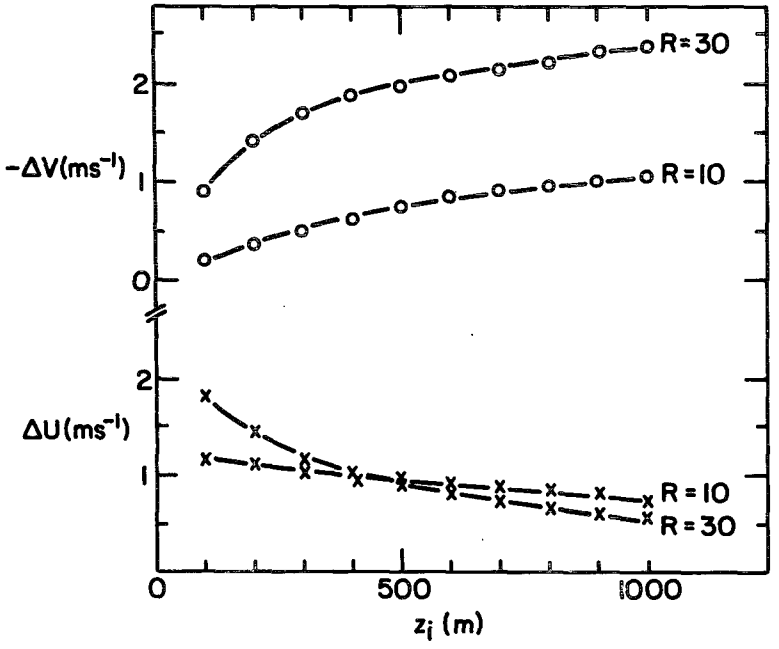

FIG. 8. Wind shear components under equilibrium conditions for a factor of 2 increase in C_N^2 due to wind shear as a function of z_i with $W_* = 1.0$ m s^{-1} and $R/S = 0.2$.

turbulence scaling velocity from Tennekes and Driedonks (1981). Based on inversion average budget equations, expressions were obtained for the rate of dissipation of turbulent kinetic energy and the vertical velocity variance which included as variables the entrainment rate and the inversion flux Richardson number R_f. Deardorff's (1980) empirical formula relating σ_{wi} and W_e provided a closure condition to eliminate σ_{wi} and obtain an expression of W_e in the presence of wind shear. This result implies a critical value of R_f that is related to the coefficients in the pressure scrambling term of the vertical velocity variance (Launder, 1975). A critical value of $R_f = \frac{1}{2}$ results from $c_1 \approx 11$.

Given a value for wind shear and knowledge of various boundary layer scaling parameters, (39) can be used to calculate the entrainment rate. From this, the value of C_N^2 at the inversion can be obtained. Since the mixed layer formalism can also be applied to boundary layer winds (Tennekes and Driedonks, 1981), the magnitude of the wind shear can be viewed as a function of entrainment (48). Thus, a feedback mechanism (wind shear enhancement of entrainment) is present to prevent large inversion wind shears from developing (except in the presence of strong boundary layer baroclinic effects such as a sloping inversion).

The barotropic equilibrium condition was used as a crude assessment of likely wind shear conditions for a neutral marine boundary layer. Strong wind shear effects are implied when the synoptic forcing is strong ($S_g > 10$ m s^{-1}), the inversion is low ($z_i < 300$ m) or the stratification above the inversion is significantly greater than $\Delta\theta_v/z_i$ ($R/S \ll 1$).

Acknowledgments. This work was supported by the Naval Environmental Prediction Research Facility and the Naval Sea Systems Command (PMS-405). The author expresses thanks for the advice and council of Andy Goroch, Dennis Thomson and Joost Businger.

REFERENCES

Brost, R. A., J. C. Wyngaard and D. H. Lenschow, 1982: Marine stratocumulus layers. Part II: Turbulence budgets. *J. Atmos. Sci.*, **39**, 818–836.

Davidson, K. L., C. W. Fairall, P. J. Boyle and G. E. Schacher, 1984: Verification of an atmospheric mixed layer model for a coastal region. *J. Climate Appl. Meteor.*, **23**, 617–636.

Deardorff, J. W., 1974: Three-dimensional numerical study of turbulence in the entraining mixed layer. *Bound.-Layer Meteor.*, **7**, 199–226.

——, 1979: Prediction of convective mixed-layer entrainment for realistic capping inversion structure. *J. Atmos. Sci.*, **36**, 424–436.

——, 1980: Stratocumulus-capped mixed layers derived from a three-dimensional model. *Bound.-Layer Meteor.*, **18**, 495–527.

——, and G. E. Willis, 1982: Dependence of mixed-layer entrainment on shear stress and velocity jump. *J. Fluid Mech.*, **115**, 123–149.

Dubosclard, G., 1982: A SODAR study of the temperature structure parameter in the convective boundary layer. *Bound.-Layer Meteor.*, **22**, 325–334.

Fairall, C. W., 1982: An analysis of the Wyngaard–LeMone model of refractive index micrometeorological structure functions at the top of a turbulent mixed layer. Tech. Rep. NPS63-82-006CR, Naval Postgraduate School, Monterey, CA 93940, 101 pp.

——, R. Markson, G. E. Schacher and K. L. Davidson, 1980: An aircraft study of turbulence dissipation and temperature structure parameter in the unstable marine atmospheric boundary layer. *Bound.-Layer Meteor.*, **19**, 453–469.

——, K. L. Davidson and G. E. Schacher, 1982: Meteorological models for optical properties in the marine atmospheric boundary layer. *Opt. Eng.*, **21**, 847–857.

Friehe, C. A., J. C. LaRue, F. H. Champagne, C. H. Gibson and G. F. Dreyer, 1975: Effects of temperature and humidity fluctuations on the optical refractive index in the marine boundary layer. *J. Opt. Soc. Am.*, **65**, 1502–1511.

Garratt, J. R., J. C. Wyngaard and R. J. Francey, 1982: Winds in the atmospheric boundary layer—Prediction and observation. *J. Atmos. Sci.*, **39**, 1307–1316.

Gossard, E. E., 1960: Power spectra of temperature, humidity, and refractive index from aircraft and tethered balloon measurements. *IEEE Trans. Antennas Propag.*, **AP-3**, 186–201.

Kato, H., and O. M. Phillips, 1969: On the penetration of a turbulent layer into a stratified fluid. *J. Fluid Mech.*, **37**, 643–655.

Launder, B. E., 1975: On the effects of a gravitational field on the turbulent transport of heat and momentum. *J. Fluid Mech.*, **67**, 569–581.

Lenschow, D. H., J. C. Wyngaard and W. T. Pennell, 1980: Mean-field and second-moment budgets in a baroclinic, convective boundary layer. *J. Atmos. Sci.*, **37**, 1313–1326.

Lilly, D. K., 1968: Models of cloud-topped mixed layers under a strong inversion. *Quart. J. Roy. Meteor. Soc.*, **94**, 292–309.

Markson, R., J. Sedlacek and C. W. Fairall, 1981: Turbulent transport of electric charge in the marine atmospheric boundary layer. *J. Geophys. Res.*, **86**, 12115–12121.

Overland, J. E., R. M. Reynolds and C. H. Pease, 1983: A model of the atmospheric boundary layer over the marginal ice zone. *J. Geophys. Res.*, **88**, 2836–2840.

Stage, S. A., and J. A. Businger, 1981: A model of entrainment into a cloud-tapped marine boundary layer. *J. Atmos. Sci.*, **38**, 2213–2242.

Stull, R. B., 1976: The energetics of entrainment across a density interface. *J. Atmos. Sci.*, **33**, 1260–1267.

Tennekes, H., 1973: A model for the dynamics of the inversion above a convective boundary layer. *J. Atmos. Sci.*, **30**, 558–567.

——, and A. G. M. Driedonks, 1981: Basic entrainment equations for the atmospheric boundary layer. *Bound. Layer Meteor.*, **20**, 515–531.

Therry, G., and P. LaCarrere, 1983: Improving the eddy kinetic energy model for planetary boundary layer description. *Bound. Layer Met.*, **25**, 63–88.

Wesely, M. L., 1976: The combined effects of temperature and humidity fluctuations on refractive index. J. Appl. Meteor., **15**, 43–49.

Wyngaard, J. C., 1973: On surface-layer turbulence. Workshop on Micrometeorology, D. A. Haugen, Ed., Amer. Meteor. Soc. 101–149.

——, 1983: Lectures on the planetary boundary layer. *Mesoscale Meteorology-Theories, Observations, and Models.* Gal-Chen and Lilly, Eds., Reidel, Holland.

——, and M. A. LeMone, 1980: Behavior of the refractive index structure parameter in the entraining convective boundary layer. *J. Atmos. Sci.*, **35**, 1573–1585.

——, Y. Izumi and S. A. Collins, 1971: Behavior of the refractive index structure parameter near the ground. *J. Opt. Soc. Am.*, **61**, 1646–1650.

——, W. T. Pennell, D. H. Lenschow and M. A. LeMone, 1978: The temperature-humidity covariance budget in the convective boundary layer. *J. Atmos. Sci.*, **35**, 47–58.

Zilitinkevich, S. S., 1975: Comments on a paper by H. Tennekes. *J. Atmos. Sci.*, **32**, 991–995.